

MCNP-CP, an Extended Version of a General Purpose Monte Carlo N-Particle Transport Code with Radionuclide Source and Coincidence / Anticoincidence Pulse Height Tally



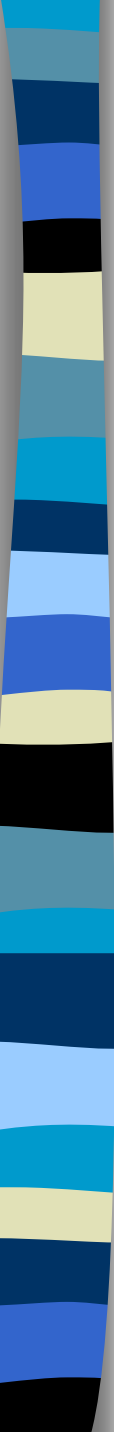
Andrey Berlizov

Institute for Nuclear Research, Kiev, Ukraine

13th UK Monte Carlo User Group Meeting MCNEG-2007

28 – 29 March, 2007

NPL, Teddington, UK



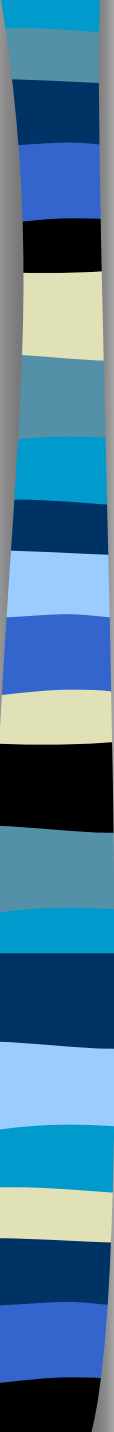
Outline

- Introduction
- MCNP-CP physics
- MCNP card extensions
- Applications
- Summary



Motivation

- Decay of radioactive nuclei and isomeric states usually represents a complex multi-stage atomic-nuclear process, which results in emission of **space and time correlated particles**: photons, β -particles, discrete energy electrons, and X-rays.
- Accurate prediction of a detection system response in measurements with such sources requires application of an **adequate source model**.



Restrictions of the standard MCNP

- Only one source particle per history is considered,
- Only source particles of particular type are considered within a calculation run, and
- There are no standard means for calculating pulse height distributions for the detection systems, which use coincidence / anticoincidence measurement techniques.

Background publications

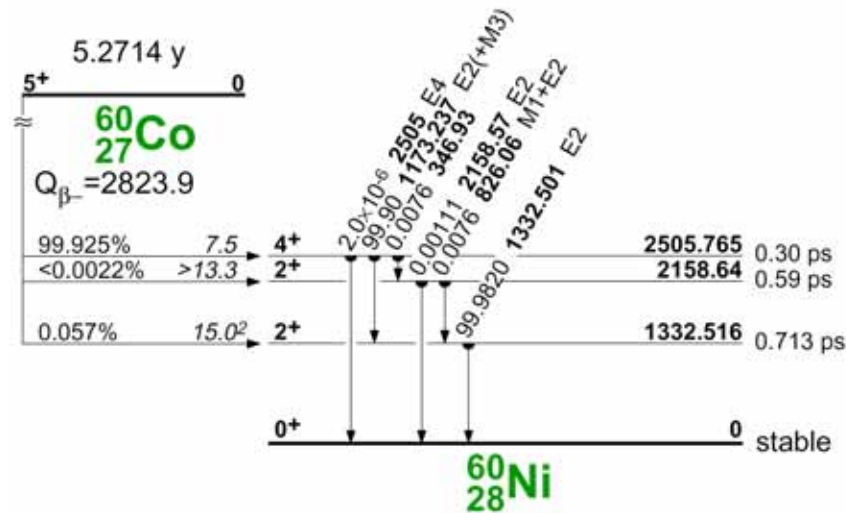
- **A.N. Berlizov, V.V. Tryshyn** / ENSDF Based Radionuclide Source for MCNP // Proceedings of the International Conference on Supercomputing in Nuclear Applications, SNA'2003, 22-24 September 2003, Paris, France.
- **A.N. Berlizov** / An upgraded multidetector pulse height tally for MCNP // Proceedings of the Monte Carlo 2005 Topical Meeting, Chattanooga, USA, April 17-21, 2005, ISBN:0-89448-695-0, American Nuclear Society, Inc.
- **A.N. Berlizov** / MCNP-CP, a Correlated Particle Radiation Source Extension of a General Purpose Monte Carlo N-Particle Transport Code // Applied Modeling and Computations in Nuclear Science. T.M. Semkow, S. Pomme, and S.M. Jerome, Eds. ACS Symposium Series 945. American Chemical Society, Washington, DC, 2006, p.183-194.

For modeling radionuclide source MCNP-CP uses:

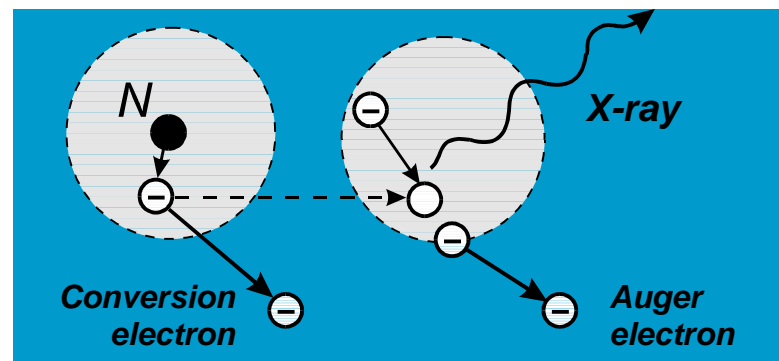
- **Evaluated Nuclear Structure Data File ENSDF** as a basic source of information about decay properties of radionuclides.
- **Known theoretical models and additional nuclear and atomic data** for simulating:
 - spectral distributions of β -particles from β^- -decay;
 - vacancy creation on the atomic K-shell and $L_{1,2,3}$ -subshells in the electron capture and internal conversion processes;
 - emission of a pair of annihilation 511-keV photons in β^+ -decay;
 - Doppler shifting of annihilation photon energies and directions;
 - intra-atomic transitions resulting in the emission of K- and LX-rays in single and double X-ray fluorescence, emission of K-LX and K-MX Auger-electrons;
 - γ - γ angular correlations of cascade γ -rays.

Electromagnetic transitions

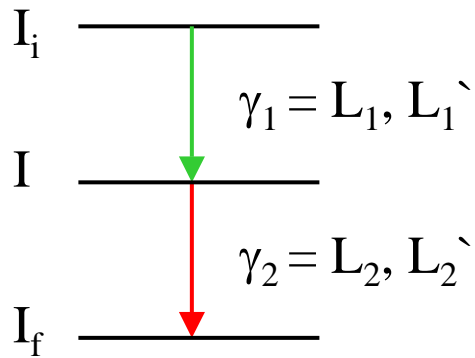
- Cascades of electromagnetic transitions are modeled based on the decay scheme information taken from the ENSDF data file.



- In each transition two competing decay modes are considered: the emission of a gamma-ray and the emission of a conversion electron from the atomic K-shells or L_{1,2,3}-subshells.



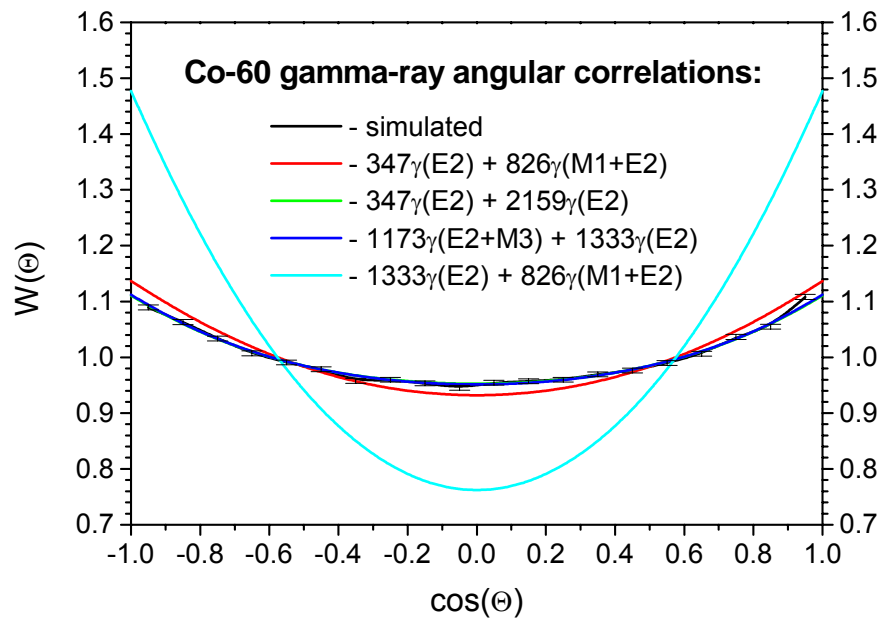
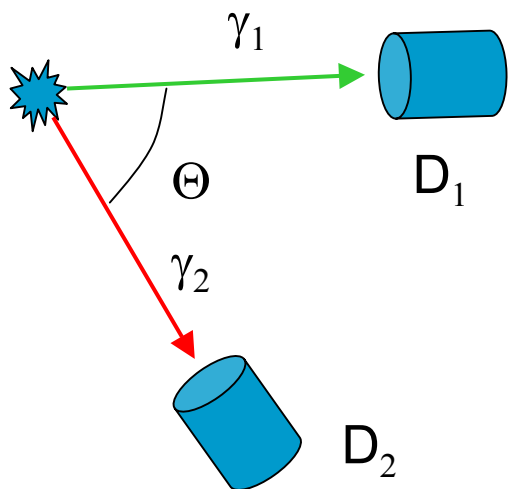
Angular correlations of cascade gamma-rays



$$W(\Theta) = 1 + \sum_{k=2}^{k_{\max}} A_{kk} P_k(\cos \Theta)$$

k – even integer number:

$$k_{\max} = \min(L_1 + L'_1, L_2 + L'_2, 2I)$$



Modeling energy distributions of β^- -particles

Beta spectrum:

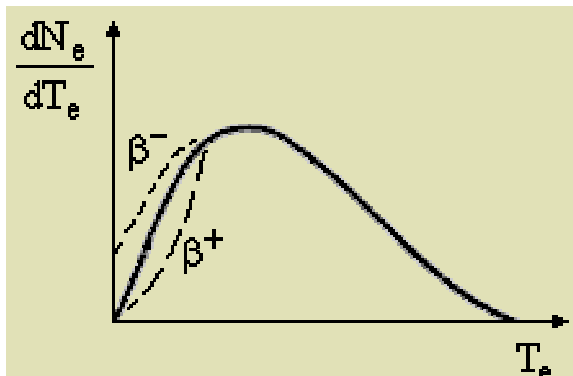
$$dN_e(Q_\beta, T_e) \propto |M_{fi}|^2 (T_e(T_e + 2m_e c^2))^{1/2} (T_e + m_e c^2)(Q_\beta - T_e)^2 F(T_e, Z) dT_e$$

Nuclear matrix element:

$$M_{fi} = G \int \phi_f^* \phi_i \exp(-i(p+q)r/\hbar) dr$$

- non-unique transitions: $|M_{fi}|^2 \sim 1$
- unique transitions: $|M_{fi}|^2 \sim p^2 + (Q_\beta - T_e)^2$

Coulomb interaction of a beta-particle with a nucleus:



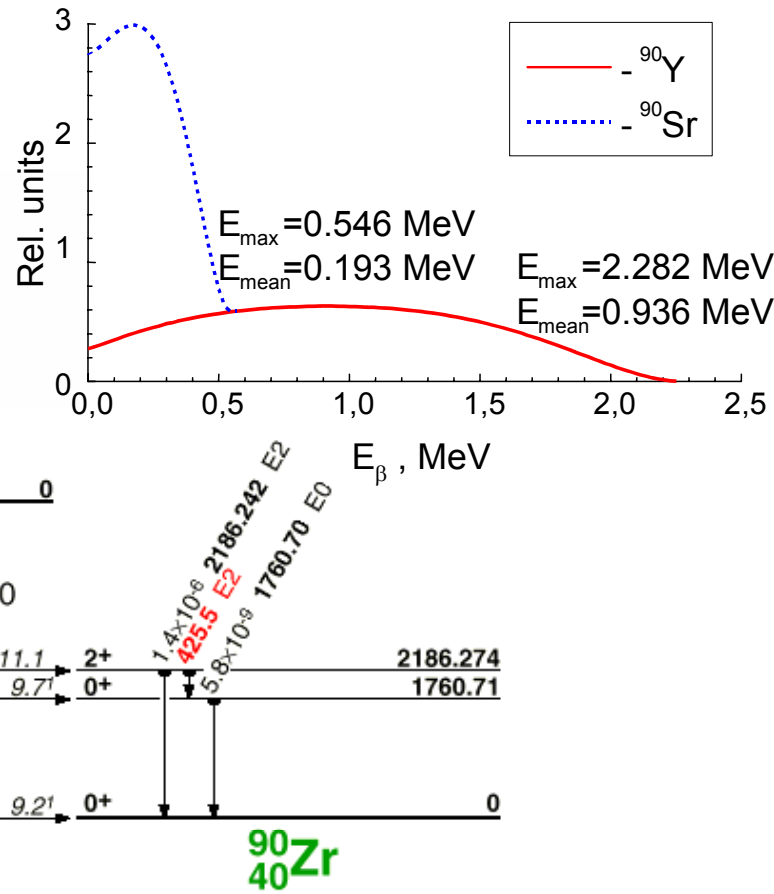
*Point nucleus approximation
(non-relativistic approach):*

$$F(T_e, Z) = \frac{2\pi\eta}{1 - \exp(-2\pi\eta)} \quad \eta = \pm \frac{\alpha Z(T_e + m_e c^2)}{pc}$$

β^- -particle energy distributions: ^{90}Sr - ^{90}Y source

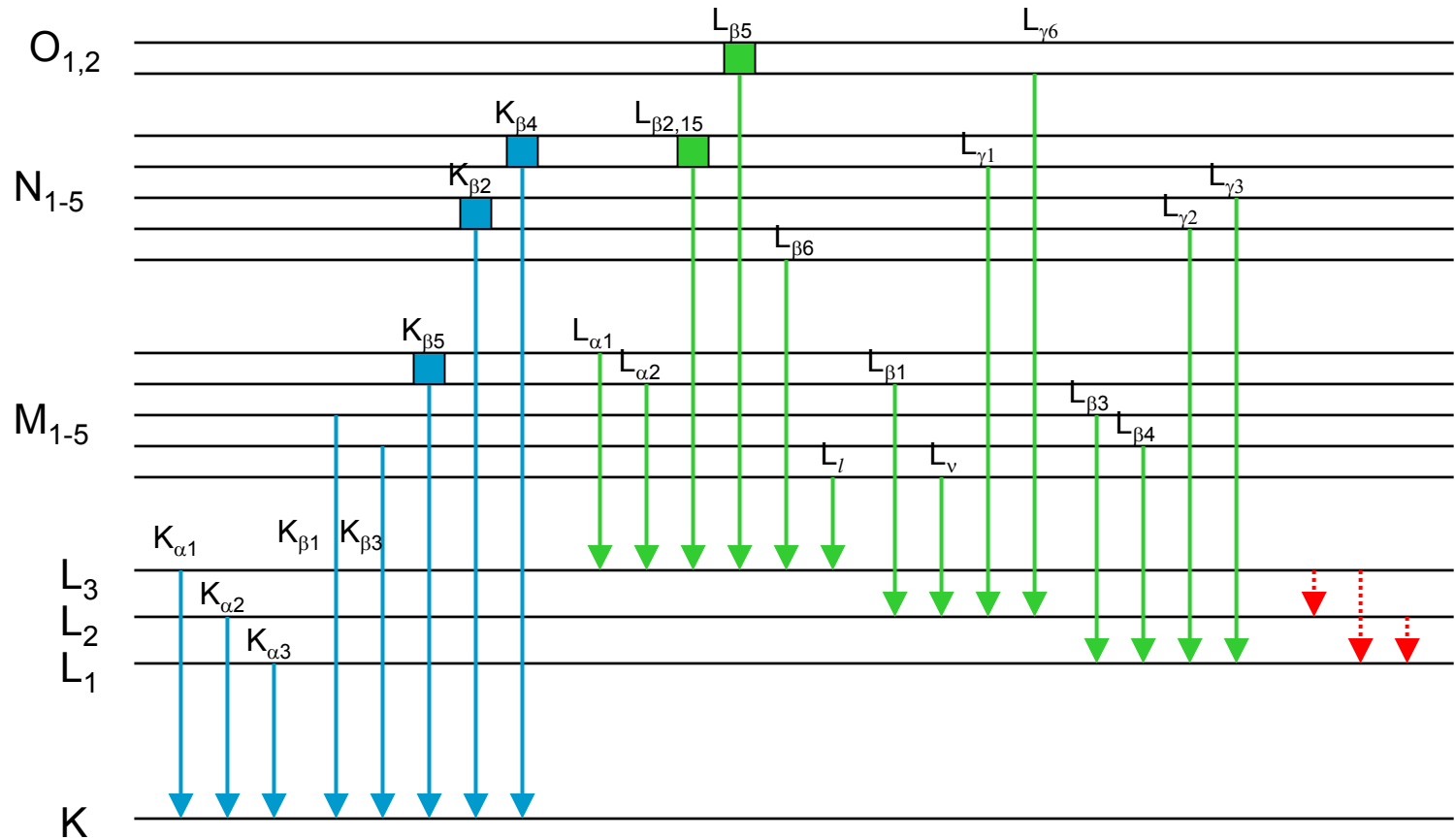
28.78 y
 0^+ — 0
 \approx
 ^{90}Sr
 38
 $Q_{\beta^-} = 546.2$

100% — 9.4^1
 2^- — 0
 \approx
 ^{90}Y
 39
 $Q_{\beta^-} = 2282.0$
 $1.4 \times 10^{-6}\%$ — 11.1
 0.0115% — 9.7^1
 2^+ — 0+
 0^+
 99.9885% — 9.2^1
 0^+ — 0



Modeling of intra-atomic transitions

X-ray and Koster-Cronig transitions taken into consideration:



Emission of Auger electrons

Following 54 Auger transitions are taken into consideration:

K-L₁X: K-L₁L₁ K-L₁L₂ K-L₁M₁ K-L₁M₂ K-L₁M₃ K-L₁M₄ K-L₁M₅ K-L₁N₁
K-L₁N₂ K-L₁N₃ K-L₁O₁ K-L₁O₂ K-L₁O₃

K-L₂X: K-L₂L₂ K-L₂L₃ K-L₂M₁ K-L₂M₂ K-L₂M₃ K-L₂M₄ K-L₂M₅ K-L₂N₁
K-L₂N₂ K-L₂N₃ K-L₂O₁ K-L₂O₃

K-L₃X: K-L₃L₃ K-L₃M₁ K-L₃M₂ K-L₃M₃ K-L₃M₄ K-L₃M₅ K-L₃N₁ K-L₃N₂
K-L₃N₃ K-L₃N₄ K-L₃N₅ K-L₃O₁ K-L₃O₂ K-L₃O₃

K-M₁X: K-M₁M₁ K-M₁M₂ K-M₁M₃ K-M₁N₁ K-M₁N₂ K-M₁N₃

K-M₂X: K-M₂M₃ K-M₂N₁ K-M₂N₃

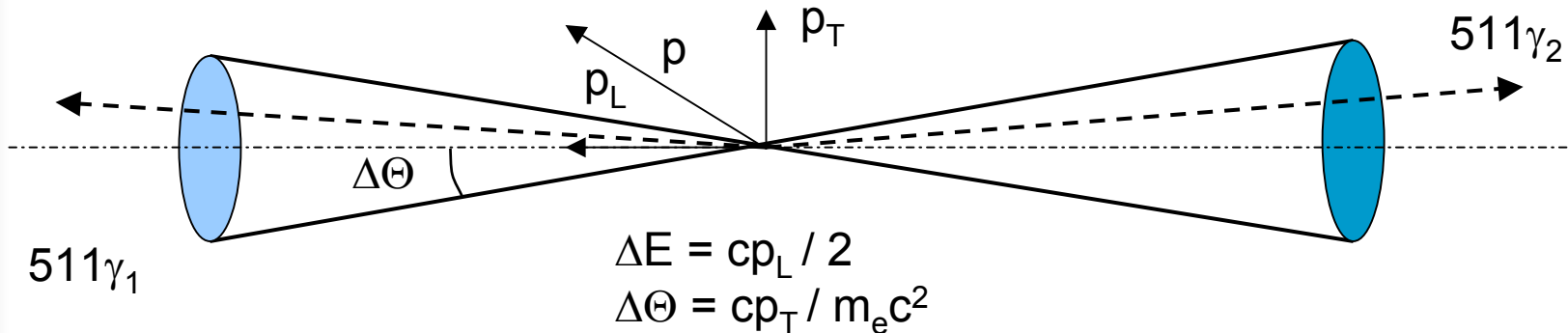
K-M₃X: K-M₃M₃ K-M₃M₄ K-M₃M₅ K-M₃N₁ K-M₃N₂ K-M₃N₃

Auger electron energies: $E(K-LX) = B_K - B_L - B_X$, $E(K-MX) = B_K - B_M - B_X$

Emission probabilities: M.O. Krause (*J. Phys. Chem. Ref. Data*, 8, 1979)

Annihilation photon emission

- Probability of emission of a pair of annihilation 511-keV photons is evaluated assuming local deposition of kinetic energy of a positron and by neglecting the on-the-fly annihilation process.
- Energies and directions of the annihilation photons are subject to Doppler shifting in the course of simulation based on the evaluations of Prochazka (*Materials Structure*, 8, No.2 (2001) 55) :



$$E_{12} = 511 \pm \sigma_E, \sigma_E = 1 \text{ keV}$$

$$\Theta = \pi \pm \sigma_\Theta, \sigma_\Theta = 2 \Delta E / m_e c^2 = 0.0039 \text{ radians (liquids and gases).}$$

General source card extension

SDEF ... ZAM=zzzaam ...

zzzaam = zzz - atomic number (nucleus charge),
aaa - mass number, and
m - isomeric index of the radionuclide of interest.
... = standard SDEF card parameters specifying source
location and geometry: CEL, SUR, X, Y, Z, POS,
EXT, RAD, AXS, CCC.

Default: zzzaaam = 0000000, which results in standard SDEF
card function.

Example: SDEF POS=0 0 0 ZAM=270600
 ^{60}Co point source ($Z = 27$, $A = 60$, $M = \text{ground state}$)
located at the origin of a coordinate system

Source settings card

CPS	RT	IAS	IGA	IAN	IKX	ILX	IBT	ICE	IAE	IGG
-----	----	-----	-----	-----	-----	-----	-----	-----	-----	-----

RT	= the correlated particle grouping time in shakes.
IAS	= analog/semi-analog decay simulation flag.
IGA	= decay gamma-ray emission flag.
IAN	= annihilation photon emission flag.
IKX	= KX-ray emission flag.
ILX	= LX-ray emission flag.
IBT	= beta-particles emission flag.
ICE	= conversion electrons emission flag.
IAE	= Auger electrons emission flag.
IGG	= gamma-gamma angular correlation flag.

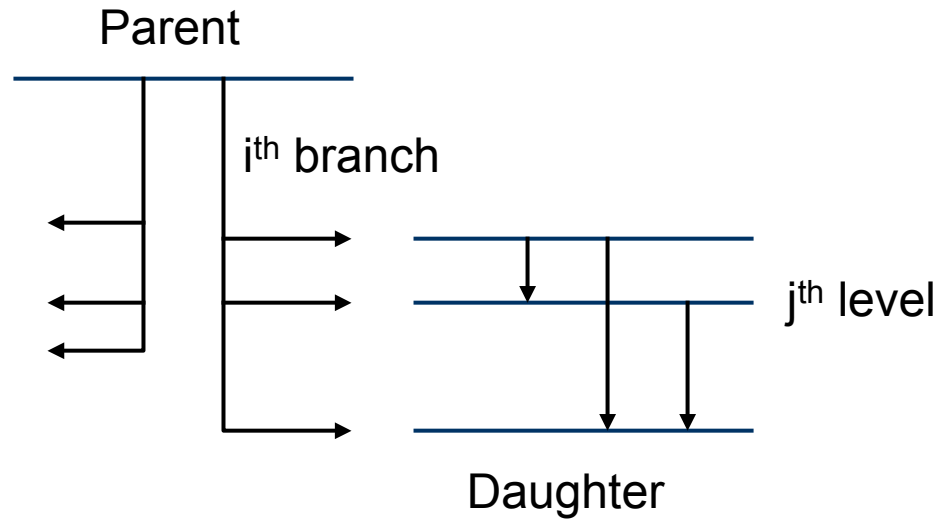
Default: RT=50 IAS=IGA=IAN=IKX=ILX=IBT=ICE=IAE=IGG=1.

Use: Use IGA through IAE entries to enable (0) or disable (1) emission of different types of particles. Zero value of IGG flag suppresses modeling of gamma-gamma angular correlations.

CPS card: Source simulation modes

- **$RT > 0$:** particles are grouped within the time intervals with length RT according to their emission times. Then each of the particle groups are tracked in different histories (one history per group), thus assuming no correlations between groups. This mode can be considered as a realistic source mode.
- **$RT = 0$:** all particles are considered within one group (and within one history) disregarding their emission times, the so called forced correlation case.
- **$RT = -1$:** particles are sampled in the same manner as it is done in two previous modes, but each particle is tracked in a separate history disregarding its emission time. This is so called forced uncorrelated source mode.
- **$RT < 0$ ($RT \neq -1$):** all particles are sampled independently using per-decay probabilities. Tracking of particles is carried out in separate histories, one history per one particle. This is the case of totally uncorrelated source.

IAS flag: analog / semi-analog source simulation modes



Analog (IAS=1)

$$P_{ij} = BR_i \cdot PP_j$$
$$wgt_{ij} = 1$$

Semi-analog (IAS=0)

$$P_{ij} = 1$$
$$wgt_{ij} = BR_i \cdot PP_j$$

P_{ij} - probability of population of level “j” through decay branch “i”,
 BR_i – branching ratio for decay branch “i”,
 PP_j – population probability for level “j”,
 wgt_{ij} - particle weights assigned when simulating the decay.

Extended pulse-height tally F8

Fn:p1 bin₁ bin₂ ... bin_M

n = tally number (8, 18, 28 ...).

p1 = P, E or P,E.

M = number of tally bins.

bin_i = *i*-th tally cell bin.

All standard formats of cell bins remained supported:

- single cell - bin = S, where S is problem number of cell for tallying;
- cell union - bin = (S₁ S₂ ... S_N);
- rep. structure and lattice tally - bin = ((S₁ S₂) < (C₁ C₂[I₁ ... I₂]) < (C₃ C₄ C₅)).

New Coincidence / Anticoincidence tally bin format:

bin = ((S₁ ... S_I) + (C₁₁ ... C_{1J1}) ... -(A₁₁ ... A_{1K1}) ...)

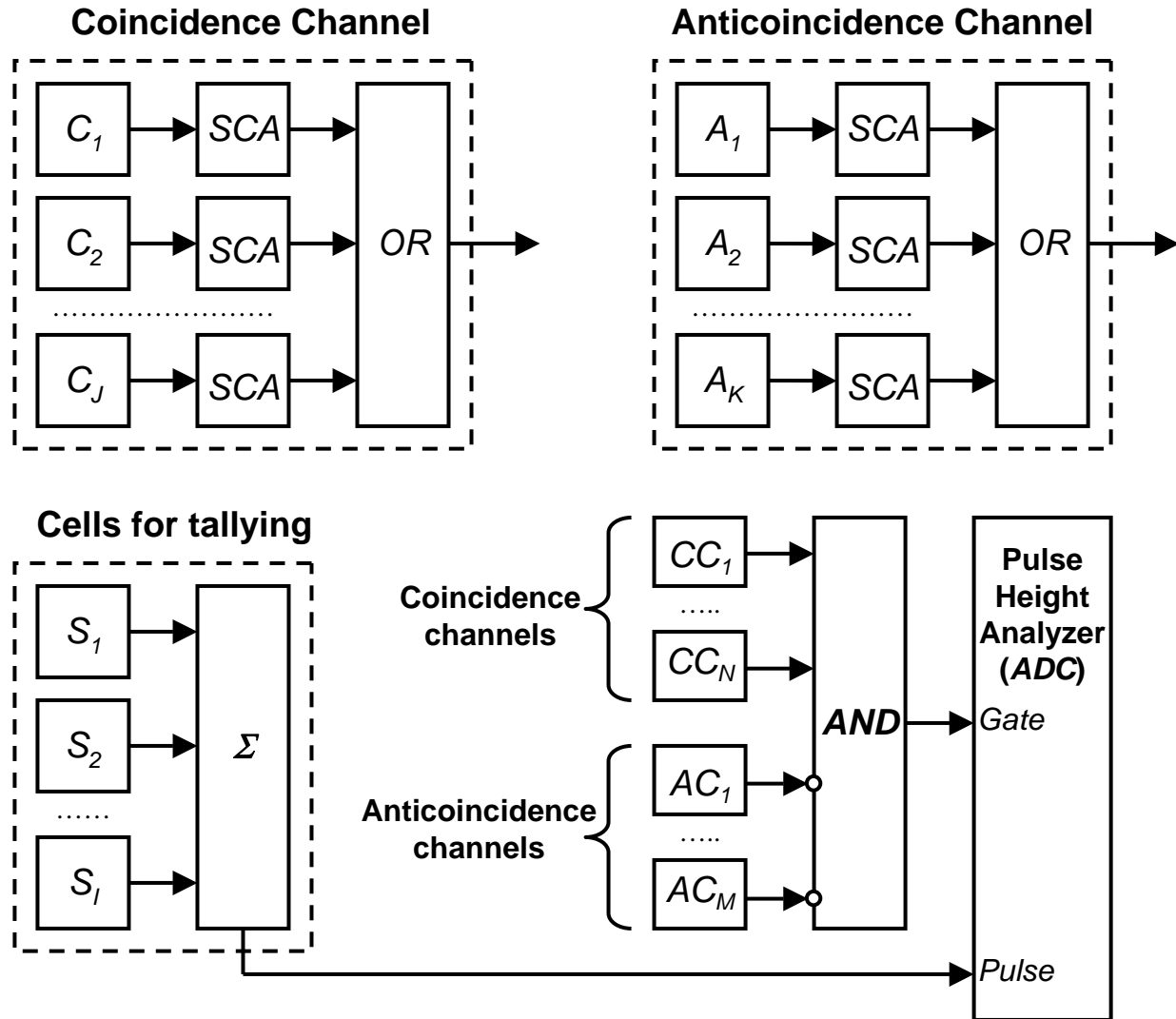
{

Cells for
tallying

{

Tallying condition

Logic of tallying of a coincidence / anticoincidence cell bin



MCNP-CP output

1decay branch: Eu-152 EC Sm-152 (13.54 y) - 72.08%

print table 210

Exited and ground level properties

##	Level E,keV	Spin & Parity		Half Life	Transition intensities *				Flag **
		ENSDF2	Taken as		Beta-	Beta+	EC	Alpha	
1	0.000	0+	0+	stable	0.0000	0.0000	0.0000	0.0000	A/NQ
2	121.782	2+	2+	1.396 NS	0.0000	0.0110	0.7421	0.0000	A/NQ
3	366.479	4+	4+	60 PS	0.0000	0.0028	0.9025	0.0000	A/NQ
4	684.701	0+	0+		0.0000	0.0000	0.0000	0.0000	A/NQ
5	706.880	6+	6+		0.0000	0.0000	0.0000	0.0000	A/NQ
6	810.453	2+	2+	7 PS	0.0000	0.0000	1.3036	0.0000	A/NQ
7	963.354	1-	1-		0.0000	0.0000	0.0000	0.0000	A/NQ
8	1022.966	4+	4+		0.0000	0.0000	0.2377	0.0000	A/NQ
9	1041.114	3-	3-	5 PS	0.0000	0.0000	0.0762	0.0000	A/NQ
10	1085.883	2+	2+	4 PS	0.0000	0.0000	21.7903	0.0000	A/NQ
11	1233.855	3+	3+	6 PS	0.0000	0.0000	17.4583	0.0000	A/NQ
12	1292.757	(2+)	2+		0.0000	0.0000	0.6598	0.0000	A/NQ
13	1371.744	4+	4+		0.0000	0.0000	0.8614	0.0000	A/NQ
14	1529.794	2-	2-	27 FS	0.0000	0.0000	24.9892	0.0000	A/NQ
15	1579.432	3-	3-		0.0000	0.0000	2.0908	0.0000	A/NQ
16	1612.780	4+,5-	4+		0.0000	0.0000	0.0212	0.0000	A/Q
17	1649.889	2-	2-		0.0000	0.0000	0.9256	0.0000	A/NQ
18	1730.240	(3-)	3-		0.0000	0.0000	0.0424	0.0000	A/NQ
19	1757.032	2+,3+	2+		0.0000	0.0000	0.0471	0.0000	A/NQ
20	1769.100	2+	2+		0.0000	0.0000	0.0662	0.0000	A/NQ

* Intensities per 100 decays of a parent nucleus.

** Adopted, NonAdopted, Questionable or NonQuestionable level.

MCNP-CP output (cont'd)

Vacancies due to electron capture

##	Level E, keV	Decay Q, keV	Unique ness	Intensity of vacancies on atomic shells			
				K-shell	L1-shell	L2-shell	L3-shell
1	0.000	1874.300		0.00e+000	0.00e+000	0.00e+000	0.00e+000
2	121.782	1752.518		6.25e-001	8.78e-002	3.40e-003	5.42e-005
3	366.479	1507.821		7.59e-001	1.07e-001	4.15e-003	8.33e-005
4	684.701	1189.599		0.00e+000	0.00e+000	0.00e+000	0.00e+000
5	706.880	1167.420		0.00e+000	0.00e+000	0.00e+000	0.00e+000
6	810.453	1063.847		1.09e+000	1.56e-001	6.05e-003	2.00e-004
7	963.354	910.946		0.00e+000	0.00e+000	0.00e+000	0.00e+000
8	1022.966	851.334		1.99e-001	2.87e-002	1.11e-003	4.93e-005
9	1041.114	833.186		6.39e-002	9.20e-003	3.57e-004	1.63e-005
10	1085.883	788.417		1.83e+001	2.64e+000	1.02e-001	4.99e-003
11	1233.855	640.445		1.46e+001	2.13e+000	8.24e-002	5.14e-003
12	1292.757	581.543		5.52e-001	8.06e-002	3.12e-003	2.17e-004
13	1371.744	502.556		7.20e-001	1.06e-001	4.10e-003	3.31e-004
14	1529.794	344.506		2.08e+001	3.11e+000	1.20e-001	1.37e-002
15	1579.432	294.868		1.74e+000	2.61e-001	1.01e-002	1.30e-003
16	1612.780	261.520		1.76e-002	2.65e-003	1.03e-004	1.44e-005
17	1649.889	224.411		7.69e-001	1.17e-001	4.52e-003	7.01e-004
18	1730.240	144.060		3.51e-002	5.40e-003	2.10e-004	4.12e-005
19	1757.032	117.268		3.90e-002	6.03e-003	2.34e-004	5.01e-005
20	1769.100	105.200		5.47e-002	8.49e-003	3.29e-004	7.33e-005
TOTAL :				6.04e+001	8.84e+000	3.43e-001	2.70e-002

* Intensities per 100 decays of a parent nucleus.

MCNP-CP output (cont'd)

Properties of electromagnetic transitions

Transition ##	E,keV	Level indexes		Multipolarity		Mixing ratio	Gammas *
		init	->	fin	ENSDF2	Taken as	
1	121.782	2		1	E2	E2	0.00000 28.65984
2	244.697	3		2	E2	E2	0.00000 7.60451
3	562.930	4		2	E2	E2	0.00000 0.00268
4	340.400	5		3	E2	E2	0.00000 0.03651
5	125.690	6		4	[E2]	E2	0.00000 0.01611
6	443.965	6		3	(E2)	E2	0.00000 0.32748
7	688.670	6		2	E2+M1+E0	M1	0.00000 0.85896
8	810.451	6		1	(E2)	E2	0.00000 0.32050
9	841.570	7		2	E1	E1	0.00000 0.16642
10	963.390	7		1	E1	E1	0.00000 0.13529
11	212.568	8		6	E2	E2	0.00000 0.01989
12	316.200	8		5	(E2)	E2	0.00000 0.00215
13	656.487	8		3	E2+M1+E0	M1	0.00000 0.14522
14	901.181	8		2	E2	E2	0.00000 0.08616
15	674.675	9		3	E1	E1	0.00000 0.17287
16	919.330	9		2	E1	E1	0.00000 0.42787
17	275.449	10		6	(M1)	M1	0.00000 0.03355
18	719.349	10		3	(E2)	E2	0.00000 0.27916
19	964.079	10		2	E2+M1(+E0)	M1+E2	-9.30000 14.64532
20	1085.869	10		1	E2	E2	0.00000 10.23508
21	148.010	11		10	[M1+E2]	M1	0.00000 0.03731
...

* Intensities per 100 decays of a parent nucleus.

MCNP-CP output (cont'd)

Internal conversion coefficients

Transition ##	E,keV	Total		K-shell		L-shell		Calculated ICC for subshells*		
		ENSDF2	ENSDF2	calc.*	ENSDF2	calc.*	L1	L2	L3	
1	121.782	1.17e+000	6.85e-001	6.85e-001	3.74e-001	3.74e-001	6.39e-002	1.55e-001	1.54e-001	
2	244.697	1.08e-001	8.13e-002	8.13e-002	2.08e-002	2.08e-002	8.76e-003	6.79e-003	5.29e-003	
3	562.930	9.50e-003	7.80e-003	7.80e-003	1.28e-003	1.28e-003	9.33e-004	2.21e-004	1.27e-004	
4	340.400	3.84e-002	3.04e-002	3.04e-002	6.26e-003	6.26e-003	3.44e-003	1.67e-003	1.14e-003	
5	125.690	1.04e+000	6.24e-001	6.24e-001	3.25e-001	3.25e-001	5.86e-002	1.34e-001	1.32e-001	
6	443.965	1.78e-002	1.44e-002	1.44e-002	2.60e-003	2.60e-003	1.69e-003	5.62e-004	3.49e-004	
7	688.670	4.34e-002	3.59e-002	8.42e-003	4.97e-003	1.13e-003	1.07e-003	5.58e-005	1.08e-005	
8	810.451	3.96e-003	3.32e-003	3.32e-003	4.90e-004	4.87e-004	4.01e-004	5.66e-005	2.98e-005	
9	841.570	1.44e-003	1.23e-003	1.23e-003	1.59e-004	1.59e-004	1.46e-004	6.11e-006	6.96e-006	
10	963.390	1.11e-003	9.50e-004	9.50e-004	1.22e-004	1.22e-004	1.13e-004	4.24e-006	4.90e-006	
11	212.568	1.71e-001	1.25e-001	1.25e-001	3.60e-002	3.60e-002	1.31e-002	1.26e-002	1.03e-002	
12	316.200	4.80e-002	3.76e-002	3.77e-002	8.11e-003	8.11e-003	4.23e-003	2.28e-003	1.60e-003	
13	656.487	5.68e-002	4.97e-002	9.47e-003	6.80e-003	1.28e-003	1.20e-003	6.39e-005	1.22e-005	
14	901.181	3.14e-003	2.63e-003	2.63e-003	3.80e-004	3.77e-004	3.19e-004	3.88e-005	2.01e-005	
15	674.675	2.26e-003	1.92e-003	1.93e-003	2.52e-004	2.52e-004	2.28e-004	1.13e-005	1.27e-005	
16	919.330	1.22e-003	1.04e-003	1.04e-003	1.34e-004	1.34e-004	1.23e-004	4.81e-006	5.53e-006	
17	275.449	1.03e-001	8.75e-002	8.75e-002	1.22e-002	1.22e-002	1.13e-002	7.73e-004	1.37e-004	
18	719.349	5.21e-003	4.34e-003	4.34e-003	6.60e-004	6.58e-004	5.24e-004	8.74e-005	4.71e-005	
19	964.079	2.73e-003	2.30e-003	2.30e-003	3.20e-004	3.25e-004	2.79e-004	3.05e-005	1.56e-005	
20	1085.869	2.11e-003	1.78e-003	1.78e-003	2.50e-004	2.47e-004	2.16e-004	2.04e-005	1.04e-005	
21	148.010	5.77e-001	4.30e-001	4.80e-001	1.10e-001	6.75e-002	6.19e-002	4.77e-003	8.56e-004	
22	423.450	2.70e-002	2.20e-002	2.85e-002	3.50e-003	3.90e-003	3.63e-003	2.23e-004	4.03e-005	
23	867.373	3.46e-003	2.90e-003	2.90e-003	4.20e-004	4.19e-004	3.52e-004	4.41e-005	2.27e-005	
24	1112.069	2.02e-003	1.71e-003	1.71e-003	2.40e-004	2.36e-004	2.08e-004	1.87e-005	9.46e-006	

* Calculated are from Band et al for Z=3,6,14-29 and Hager-Seltzer for Z > 29.

x denotes measured ENSDF2 values.

MCNP-CP output (cont'd)

KX-ray and associated Auger transition intensities

K-shell X-rays				Auger electrons			
Notation	E, keV	Intensity*	Intensity**	Notation	E, keV	Intensity*	Intensity**
Ka1	40.1180	4.820e+001	3.894e+001	K-L3L3	33.4018	7.720e-001	6.237e-001
Ka2	39.5224	2.660e+001	2.149e+001	K-L2L2	32.2106	7.980e-002	6.447e-002
Ka3	39.0974	6.750e-003	5.453e-003	K-L2L3	32.8062	1.590e+000	1.285e+000
Kb1	45.4144	9.120e+000	7.368e+000	K-L1L1	31.3606	6.140e-001	4.961e-001
Kb2	46.5777	3.010e+000	2.432e+000	K-L1L2	31.7856	7.940e-001	6.415e-001
Kb3	45.2935	4.710e+000	3.805e+000	K-L1L3	32.3812	7.750e-001	6.261e-001
Kb4	46.7052	1.140e+000	9.210e-001				
Kb5	45.7411	1.350e-001	1.091e-001				

* Intensities are per 100 K-shell vacancies.

** Intensities per 100 decays of a parent nucleus.

LX-ray energies and intensities

L-shell X-rays		Intensity per 100 vacancies on			Intensity
Notation	E, keV	L1-subshell	L2-subshell	L3-subshell	*
La1	5.6360	3.330e+000	1.520e+000	1.010e+001	5.499e+000
Lb2	6.5872	7.030e-001	3.200e-001	2.140e+000	1.165e+000
La2	5.6102	3.700e-001	1.690e-001	1.120e+000	6.105e-001
Lb5	0.0000	0.0000e+000	0.0000e+000	0.0000e+000	0.0000e+000
Lb6	6.3705	3.100e-002	1.410e-002	9.420e-002	5.115e-002
Ll	4.9934	1.390e-001	6.310e-002	4.210e-001	2.284e-001
Lb1	6.2058	2.240e+000	1.180e+001	0.0000e+000	3.641e+000
Ln	5.5890	5.480e-002	2.880e-001	0.0000e+000	8.919e-002
Lg1	7.1828	3.690e-001	1.940e+000	0.0000e+000	6.008e-001
Lg6	0.0000	0.0000e+000	0.0000e+000	0.0000e+000	0.0000e+000
Lb3	6.3170	3.470e+000	0.0000e+000	0.0000e+000	4.720e-001
Lb4	6.1961	2.080e+000	0.0000e+000	0.0000e+000	2.831e-001
Lg2	7.4712	6.410e-001	0.0000e+000	0.0000e+000	8.724e-002
Lg3	7.4894	9.120e-001	0.0000e+000	0.0000e+000	1.242e-001

* Intensities per 100 decays of a parent nucleus.

MCNP-CP output (cont'd)

Gamma-gamma true coincidence table*.

##	E, keV	Ten the most intense coinciding gamma-rays, keV												
1	121.78	1408.01	964.10	1112.07	244.70	867.38	443.91	1212.95	688.67	1005.26	1457.65			
2	125.75	121.78	443.91	564.01	295.94	416.03	768.98	719.34	147.97	275.43	493.55			
3	147.97	121.78	964.10	1085.88	244.70	688.67	295.94	443.97	810.45	719.40	416.03			
4	207.69	121.78	964.10	1085.88	244.70	688.67	1005.26	919.33	443.97	810.45	719.40			
5	212.51	121.78	244.70	688.67	443.97	810.45	556.47	125.75	269.79	357.13	562.92			
6	239.31	121.78	1408.01	964.10	1112.07	1085.88	244.70	867.38	443.91	688.67	295.94			
7	244.70	121.78	867.38	443.91	1212.95	1005.26	564.01	295.94	488.68	443.97	719.40			
8	251.64	121.78	244.70	919.33	674.63	357.13								
9	269.79	121.78	244.70	688.67	443.97	810.45	656.49	901.18	340.40	212.51	125.75			
10	275.43	121.78	244.70	443.91	688.67	564.01	295.94	443.97	810.45	416.03	147.97			
11	285.86	121.78	964.10	1085.88	244.70	688.67	443.97	810.45	719.40	275.43	125.75			
12	295.94	121.78	964.10	1112.07	1085.88	244.70	867.38	688.67	443.97	810.45	719.40			
13	316.09	121.78	244.70	340.40	556.47	269.79	357.13							
14	329.40	121.78	841.57	963.35	357.13									
15	330.63	121.78	244.70	919.33	674.63	207.69	385.29							
16	340.40	121.78	244.70	556.47	664.86	905.90	269.79	207.69	385.29	357.13	316.09			
17	357.13	121.78	244.70	688.67	919.33	443.97	810.45	926.28	674.63	841.57	656.49			
18	385.29	121.78	964.10	1085.88	244.70	688.67	1005.26	919.33	443.97	810.45	719.40			
19	416.03	121.78	964.10	1112.07	1085.88	244.70	867.38	688.67	443.97	810.45	719.40			
20	423.40	121.78	244.70	688.67	295.94	443.97	810.45	416.03	125.75	523.18	496.39			
21	443.97	121.78	244.70	443.91	564.01	295.94	416.03	768.98	719.34	147.97	275.43			
22	443.91	121.78	964.10	1085.88	244.70	688.67	443.97	810.45	719.40	275.43	125.75			
23	482.30	121.78	244.70	688.67	443.97	810.45	125.75	357.13	562.92					
24	488.68	121.78	244.70	919.33	674.63	239.31								
25	493.55	121.78	964.10	1085.88	244.70	688.67	443.97	810.45	719.40	275.43	125.75			
...

* 500.000 ns resolution time was assumed.

MCNP-CP output (cont'd)

Sum peaks predictions (arranged by intensity).

##	Sum-Peak, keV	Pair of gamma-rays	Intensity product	Single
1	1529.79	121.78 + 1408.01	6.04e-002	No*
2	1233.86	121.78 + 1112.07	3.92e-002	No*
3	366.48	121.78 + 244.70	2.18e-002	Yes
4	989.16	121.78 + 867.38	1.22e-002	Yes
5	565.69	121.78 + 443.91	8.11e-003	Yes
6	1334.73	121.78 + 1212.95	4.09e-003	Yes
7	1529.79	443.91 + 1085.88	2.90e-003	No*
8	688.61	244.70 + 443.91	2.15e-003	Yes
9	1127.05	121.78 + 1005.26	1.86e-003	Yes
10	1579.43	121.78 + 1457.65	1.44e-003	No*
11	685.79	121.78 + 564.01	1.41e-003	Yes
12	417.72	121.78 + 295.94	1.28e-003	Yes
13	1041.11	121.78 + 919.33	1.23e-003	Yes
14	610.46	121.78 + 488.68	1.20e-003	Yes
15	565.76	121.78 + 443.97	9.39e-004	Yes
16	1649.89	121.78 + 1528.11	8.09e-004	No*
17	841.19	121.78 + 719.40	8.00e-004	Yes
18	1048.06	121.78 + 926.28	7.98e-004	Yes
19	1260.04	295.94 + 964.10	6.56e-004	Yes
.....				

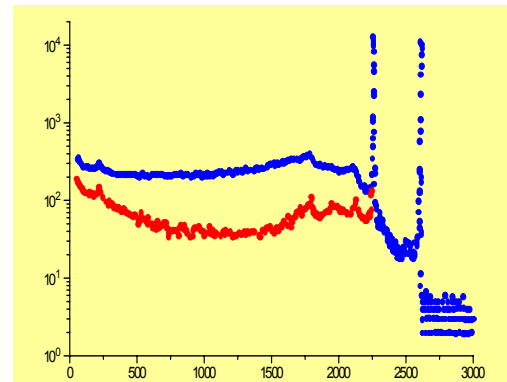
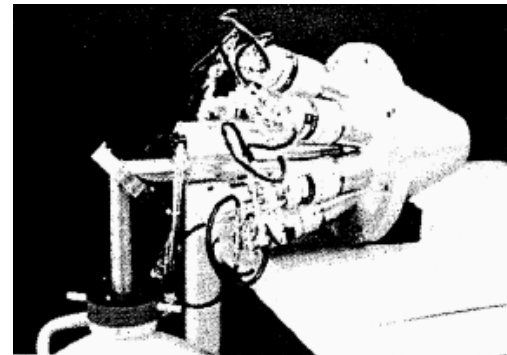
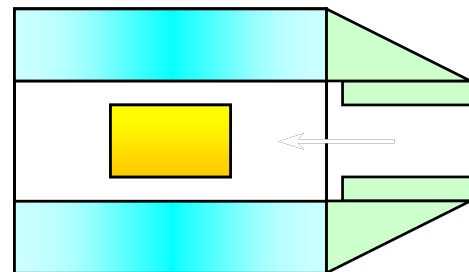
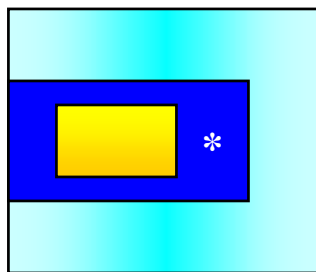
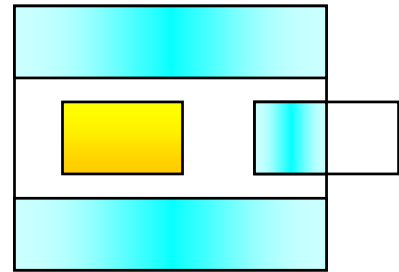
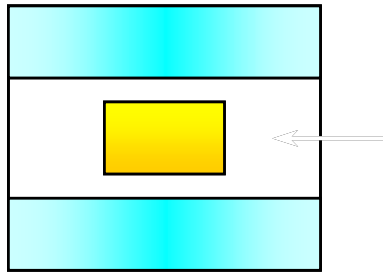
* Pair with the largest intensity product indicated.

**No pairs differing by > 100 times in intensity product included.

Possible applications

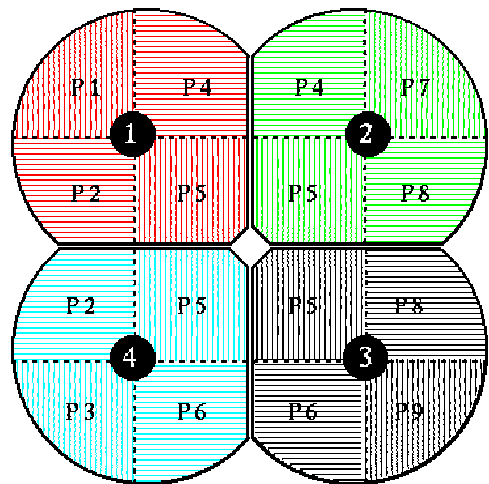
Calculation of characteristics and optimization of construction of detectors and detector systems:

- Single crystal spectrometers
- Pair Gamma-Spectrometers
- Phoswich detectors
- Compton/Escape Suppression Spectrometers



Possible applications (cont'd)

CLOVER segmented detector
NPRG at Liverpool, UK

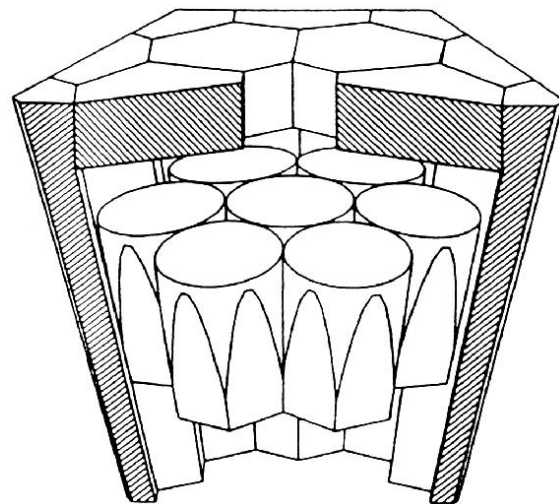


4 coaxial n-type Germanium crystals arranged like a four leaf clover. Outer p-type contact of each crystal segmented longitudinally, splitting each crystal into four quadrants.



<http://ns.ph.liv.ac.uk/>

CLUSTER detector
FZ Rossendorf, Germany



The detector comprises seven individually encapsulated HPGe crystals of about 60 % efficiency in a common cryostat surrounded by an escape-suppression shield consisting of 18 optically isolated BGO scintillator crystals.

<http://www.fz-rossendorf.de/>



Possible applications (cont'd)

GAMMASPHERE

Argonne National Laboratory, USA

The array consists of 110 large volume, high purity germanium detectors, each in a BGO (Bismuth Germanate) compton suppression shield.



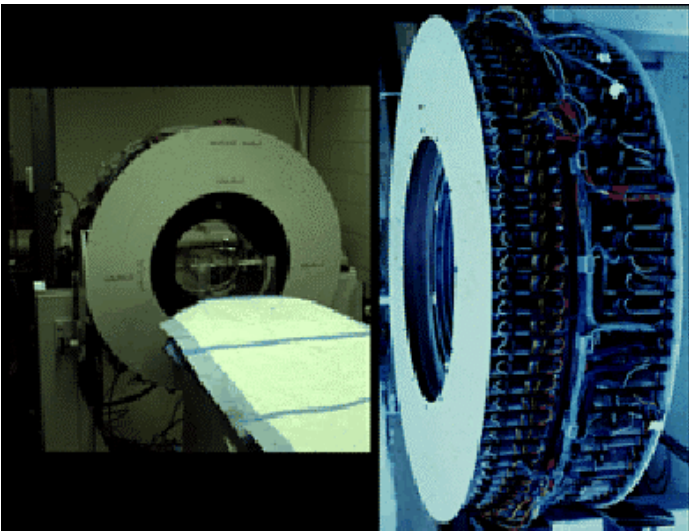
<http://www-gam.lbl.gov/>
<http://www.phy.anl.gov/gammasphere/>



ANL Physics Division

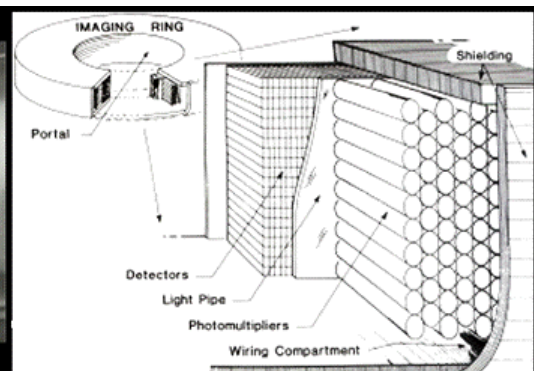
Possible applications (cont'd)

Nuclear Medical Imaging with
Positron emission tomography (PET)



PCR-I, a single ring positron emission tomograph.

Source: *A HISTORY OF POSITRON IMAGING*
by Gordon L. Brownell,
Massachusetts Institute of Technology



PCR-II, a cylindrical positron emission tomograph.

Possible applications (cont'd)

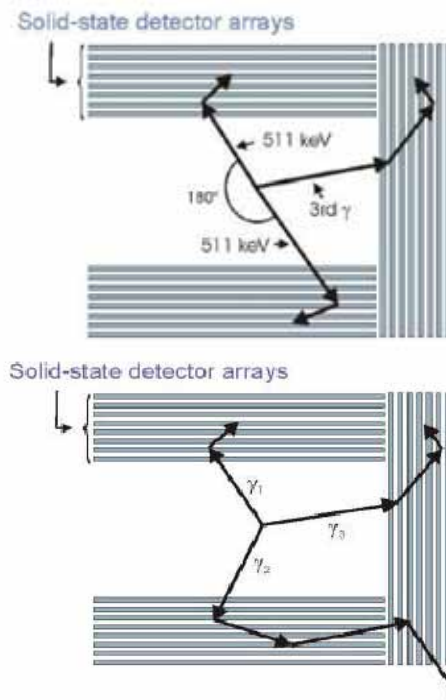
Compton Imaging System



Ring Compton camera. Scatter detector: $3 \times 3 \text{ cm}^2$ silicon pad detectors. Absorption detector: Each of eleven detector modules is nominally composed of 44 NaI(Tl) bars.

Source: *Compton Imaging System Development and Performance Assessment by Chia-ho Hua, University of Michigan, Ph.D. dissertation, 2000*

Coincident Compton Imaging

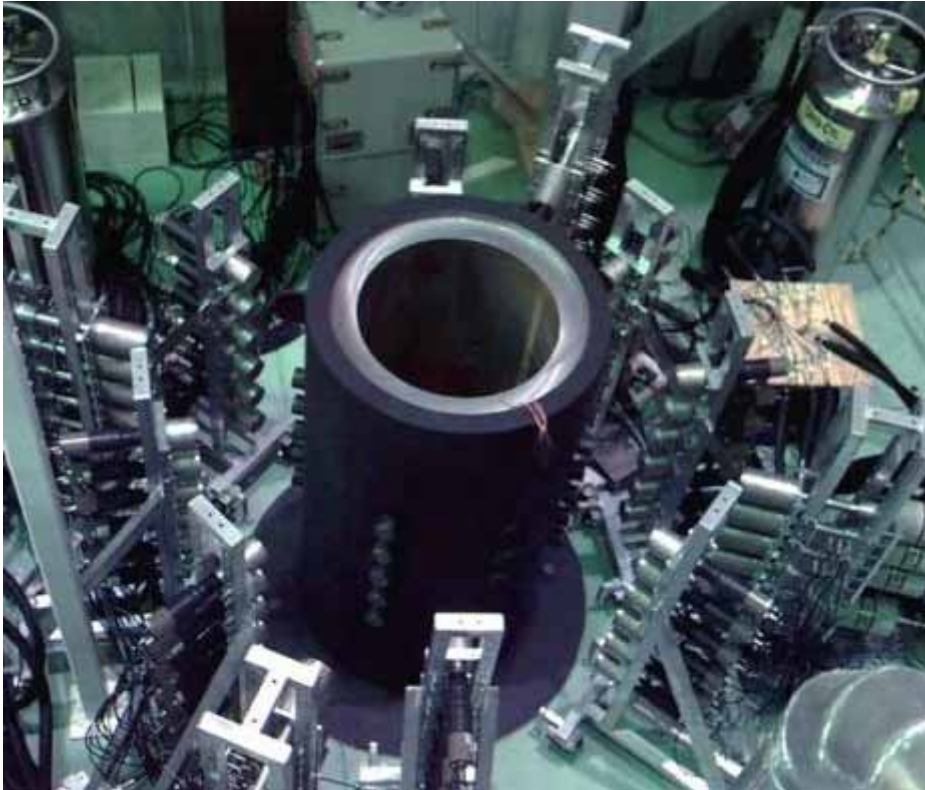


Coincident Compton imager uses a positron emitting radionuclide accompanied by an additional γ -ray (top) or 3-gamma cascade (bottom)

Source: *Coincident Compton Nuclear Medical Imager by James D. Kurfess and Bernard F. Philips Naval Research Laboratory, Washington, DC USA*

Possible applications (cont'd)

NDA techniques: Multi-Detector Analysis System for Spent Nuclear Fuel

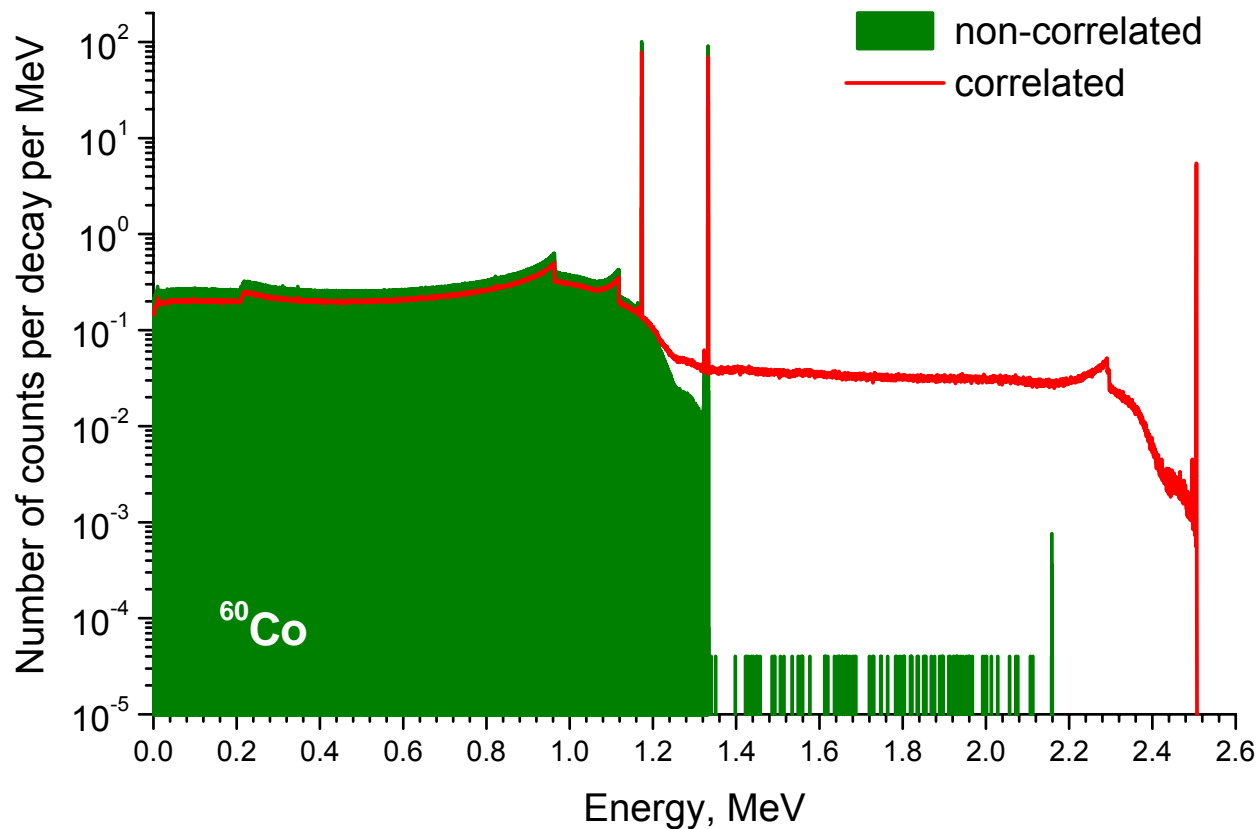


Prototype MDAS has 68 detectors; 20 HPGe for gamma-ray detection and 48 liquid scintillator detectors for neutron detection.

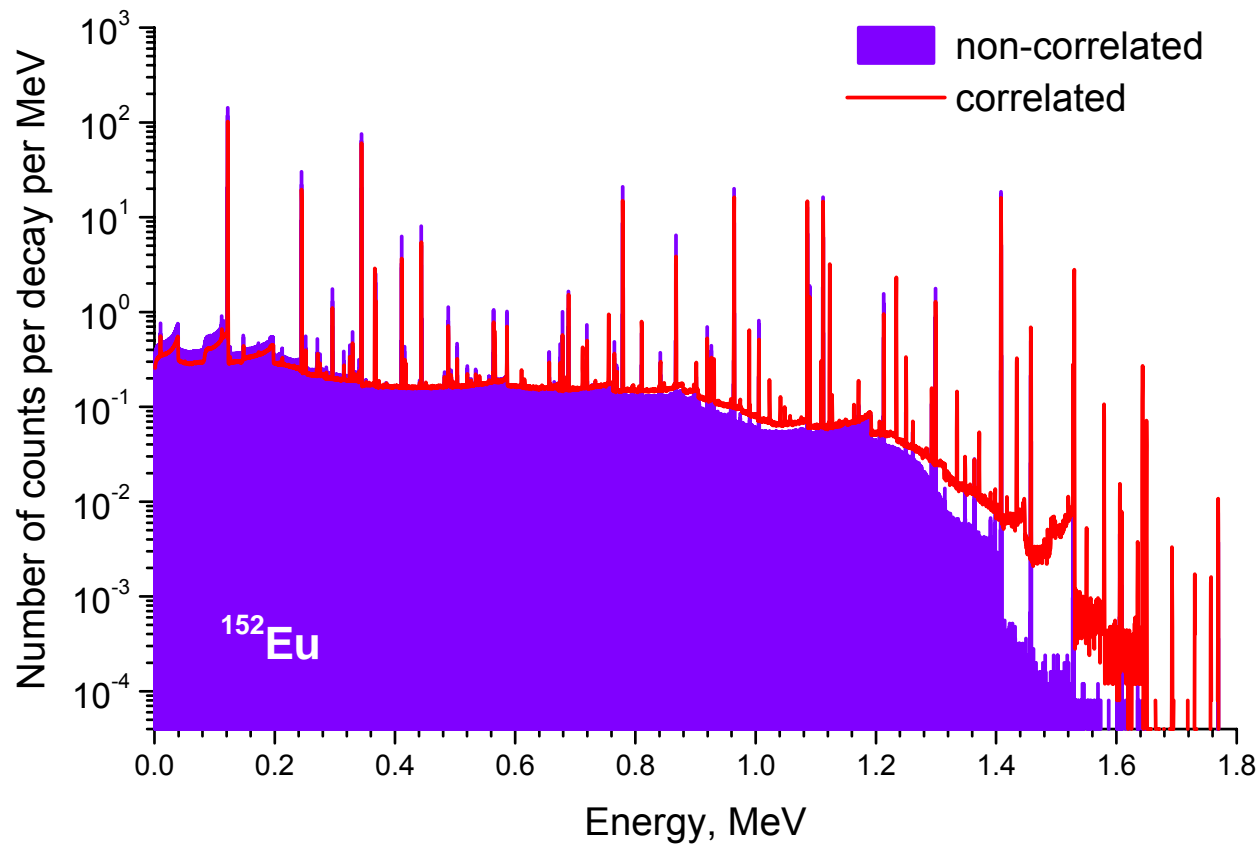
Advantages: fast coincidence methods, list-mode data, gamma-ray coincidence, neutron coincidence, pulse-shape discrimination, detector arrays, and data acquisition and analysis.

Source: Using New Fission Data with the Multi-Detector Analysis System for Spent Nuclear Fuel by J.D. Cole et al., INEEL, USA

Coaxial 60% HPGe with Co-60 point source (close geometry)

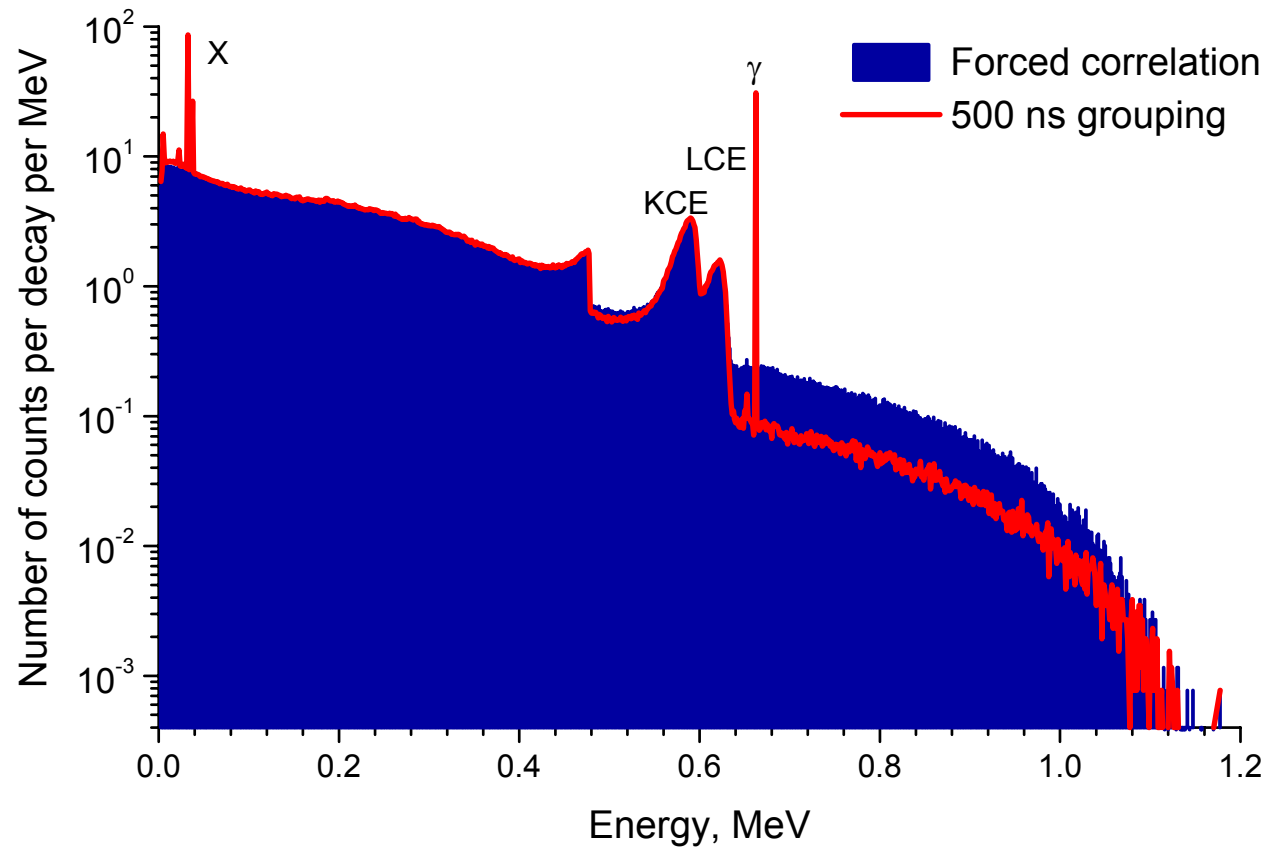


Coaxial 60% HPGe with Eu-152 point source (close geometry)

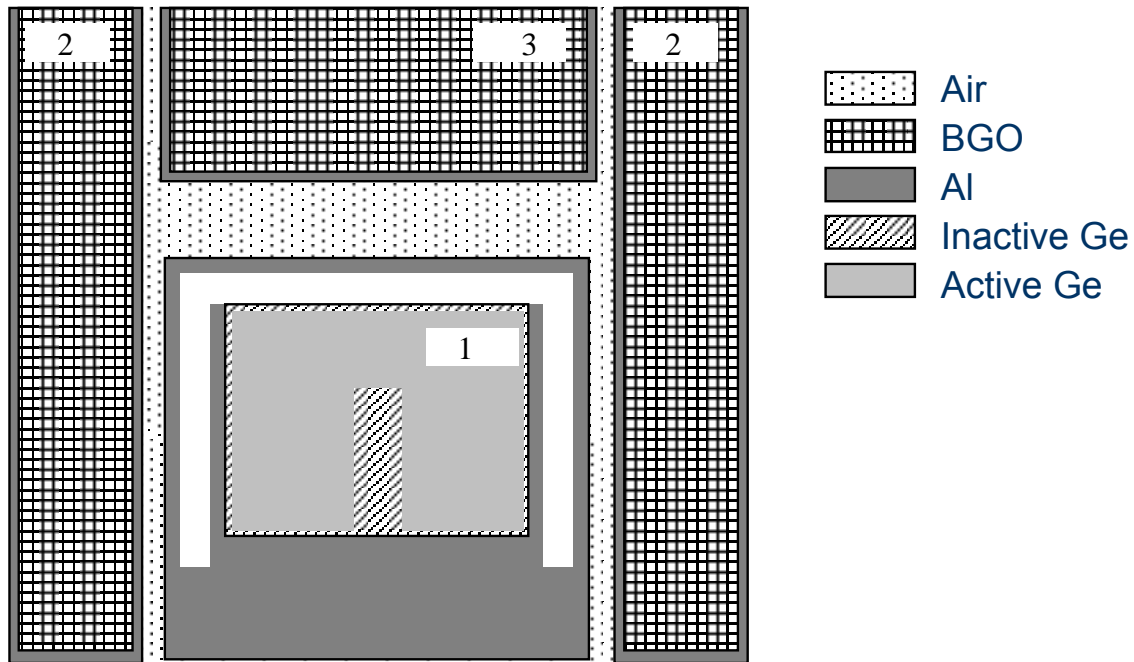


Planar LEGe Detector with Cs-137 point source

($\varnothing 16 \times 10$ mm, Inactive Ge = 0.3 μm , Be window = 0.005 in.)



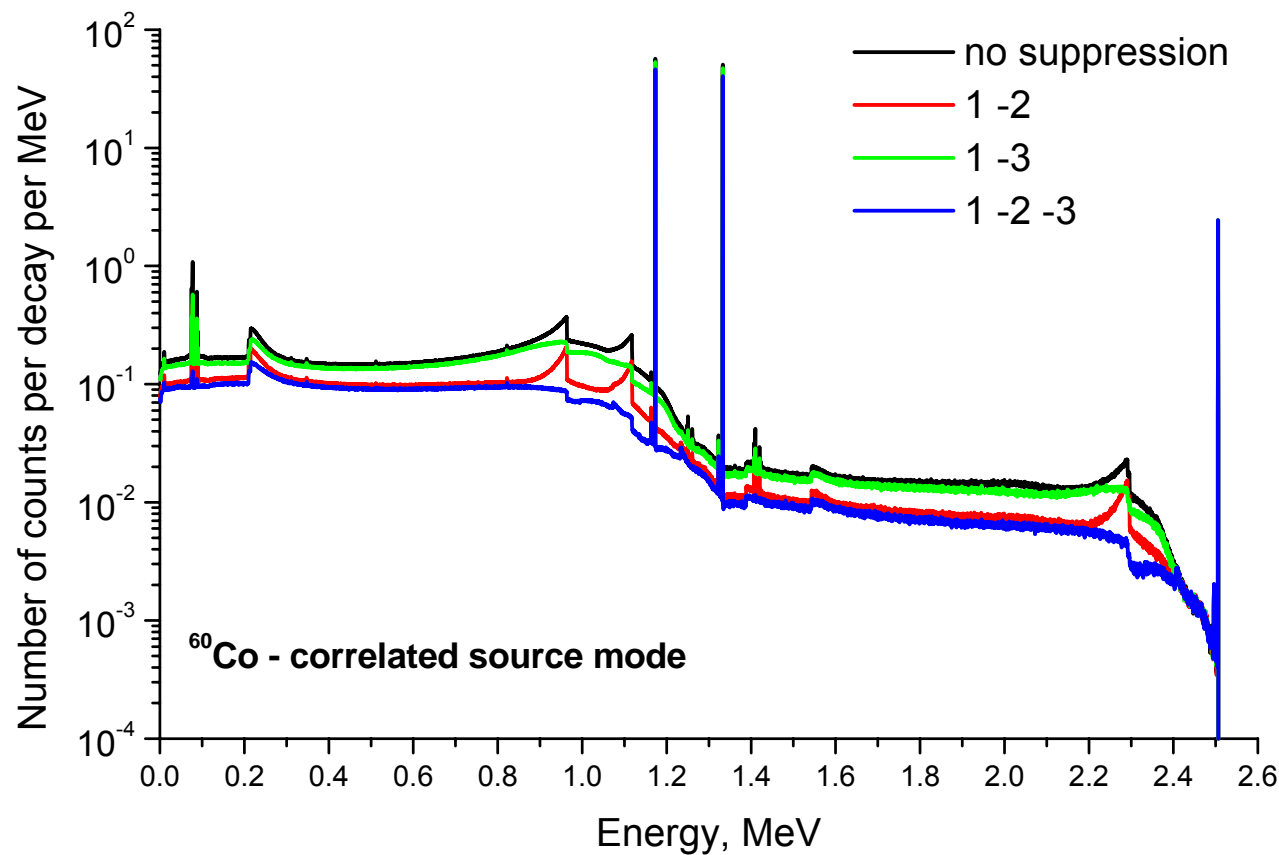
Compton Suppression Spectrometer based on coaxial 60% HPGe and BGO detectors



Analyzing detector: HPGe with relative efficiency 60%, crystal - $\varnothing 74 \times 53$ mm, inactive germanium – 0.7 mm, rear contact - $\varnothing 10 \times 36$ mm, crystal cladding – 1 mm of Al.

Guard detectors: annular and plug BGO scintillators with 1.5 mm aluminum coating and thickness 3 and 4 cm respectively.

Compton Suppression Spectrometer with Co-60 point source

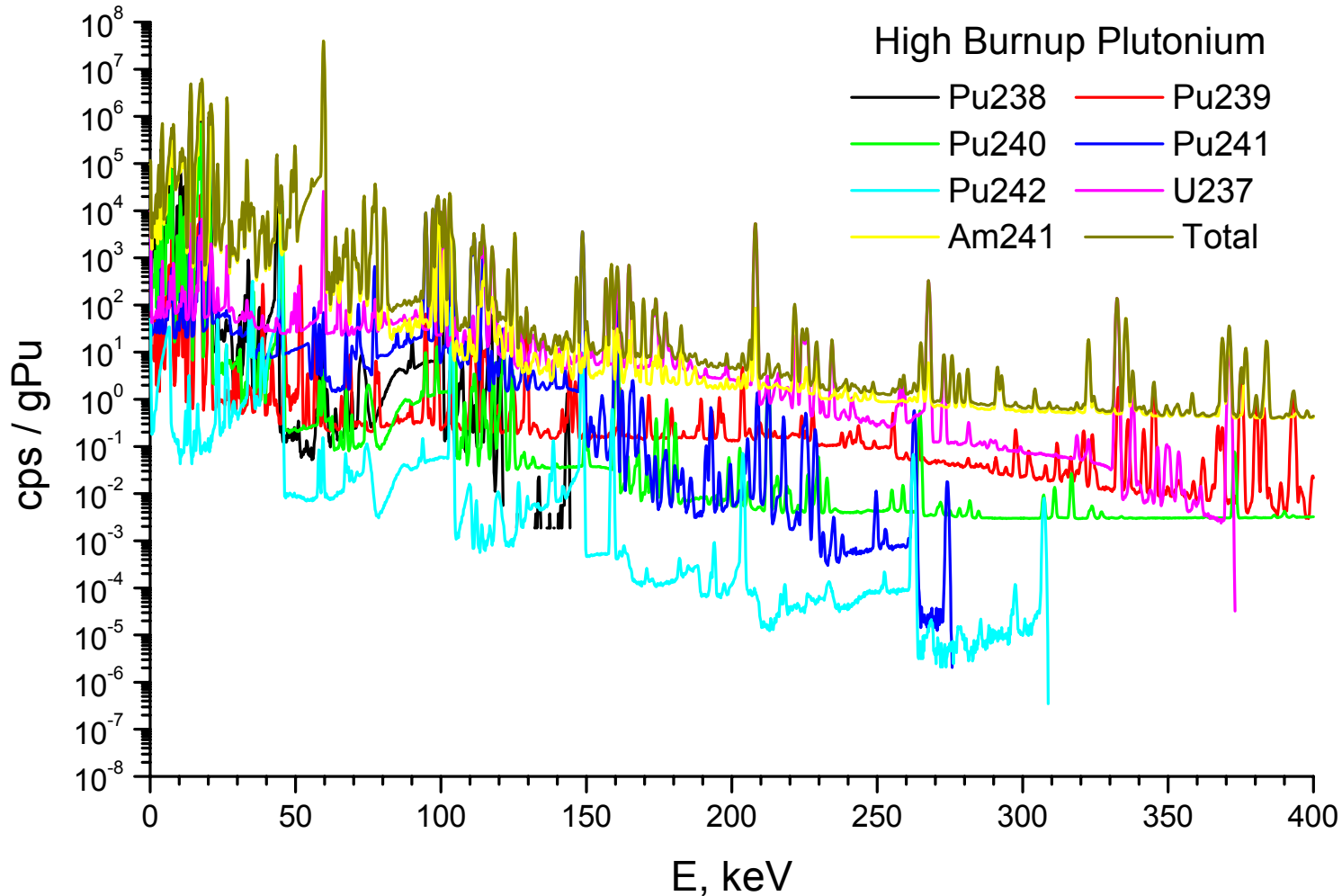


Compton Suppression Spectrometer: coincidence summing corrections calculations*

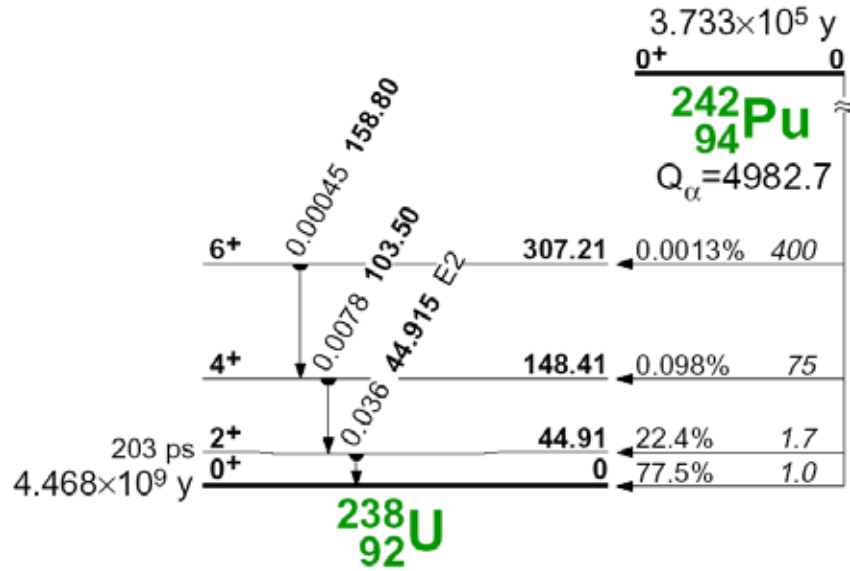
Decay branch	E_{γ} , keV	Compton Suppression Spectrometer CFs			
		no suppression	plug	annular	plug and annular
$^{60}\text{Co} \rightarrow ^{60}\text{Ni}$	1173.25	1.300	1.372	1.511	1.595
	1332.52	1.310	1.392	1.536	1.634
$^{152}\text{Eu} \rightarrow ^{152}\text{Sm}$	121.78	1.404	1.537	1.732	1.897
	244.70	1.601	1.932	2.290	2.905
	443.97	1.514	1.730	1.985	2.312
	867.37	1.743	2.562	3.716	7.614
	964.08	1.248	1.422	1.535	1.844
	1085.87	0.889	0.902	0.913	0.926
	1112.07	1.136	1.284	1.376	1.639
	1408.01	1.185	1.344	1.403	1.678
$^{152}\text{Eu} \rightarrow ^{152}\text{Gd}$	344.28	1.259	1.335	1.450	1.535
	411.12	1.758	2.269	3.140	4.493
	778.90	1.413	1.696	2.189	2.910

* A.N. Berlizov, V.V. Tryshyn, **A Monte Carlo approach to true-coincidence summing correction factor calculation for gamma-ray spectrometry applications**, Journal of Radioanalytical and Nuclear Chemistry, Vol.264, No.1 (2005) 169-174.

γ - γ coincidence technique for the direct measurement of ^{242}Pu : applicability study



Decay properties of ^{242}Pu



Possible double coincidences:

44.9 keV – 103.5 keV

44.9 keV – 158.8 keV

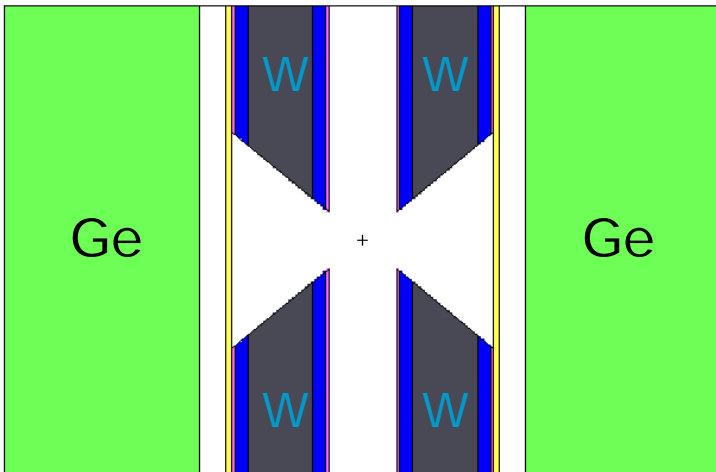
103.5 keV – 158.8 keV

most appropriate

Reasons:

1. Lower energy of 44.9 keV photons will result in higher self-attenuation.
2. Higher intensity of 44.9 keV photons will produce higher background of accidental coincidences.

Measurement setup model



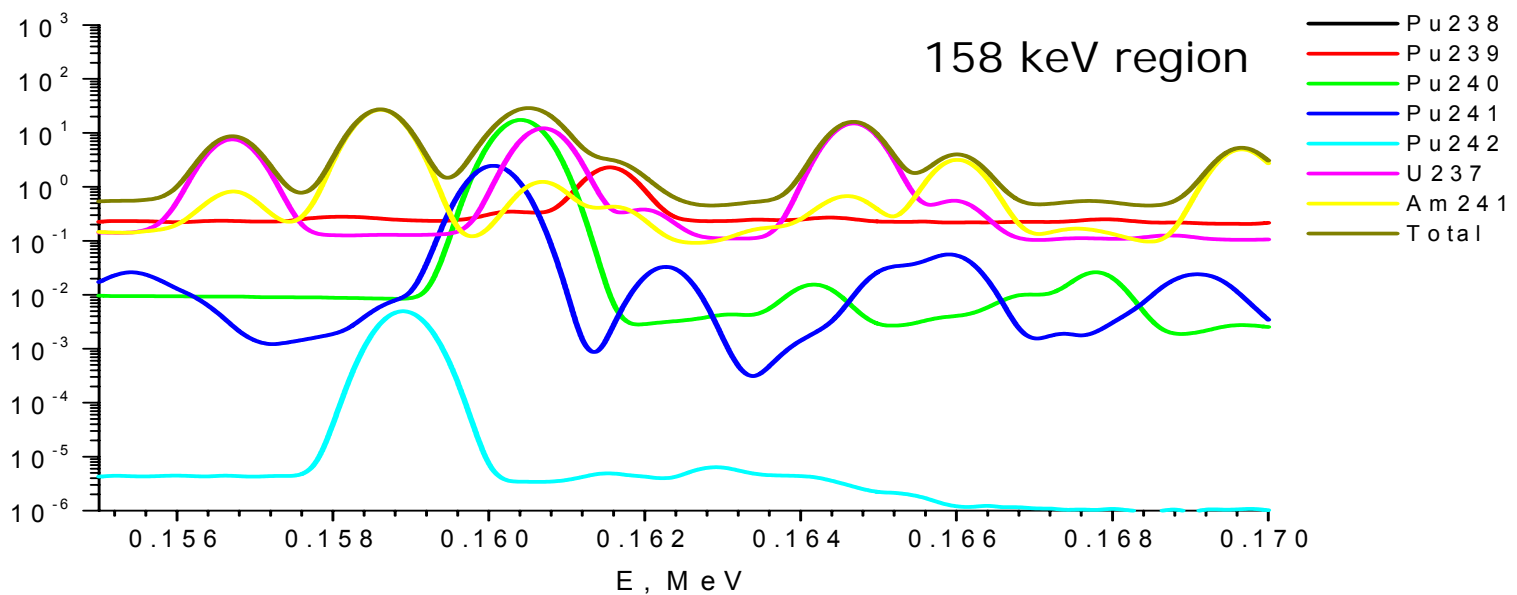
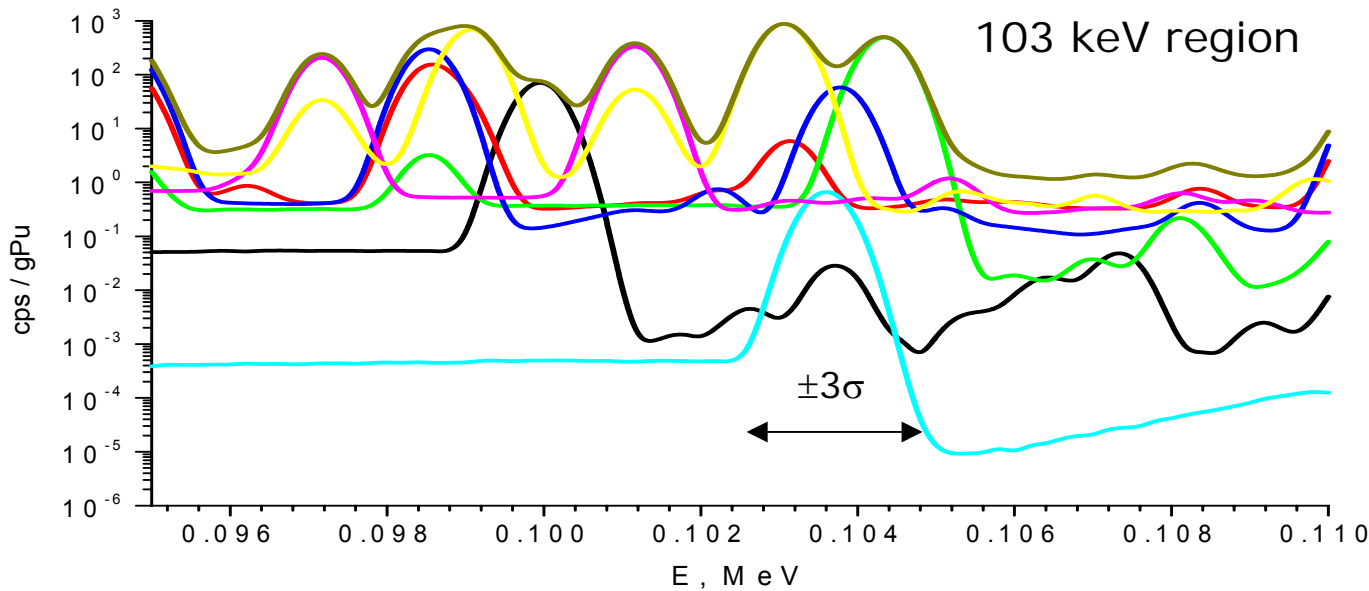
Geometry:

- Detectors: planar HPGe ($S=1000 \text{ mm}^2$, $d=15 \text{ mm}$);
- Input windows: Al (0.5 mm);
- Collimators: W (5 mm) lined with Cd (1 mm) and Cu (0.2 mm);
- Source: point

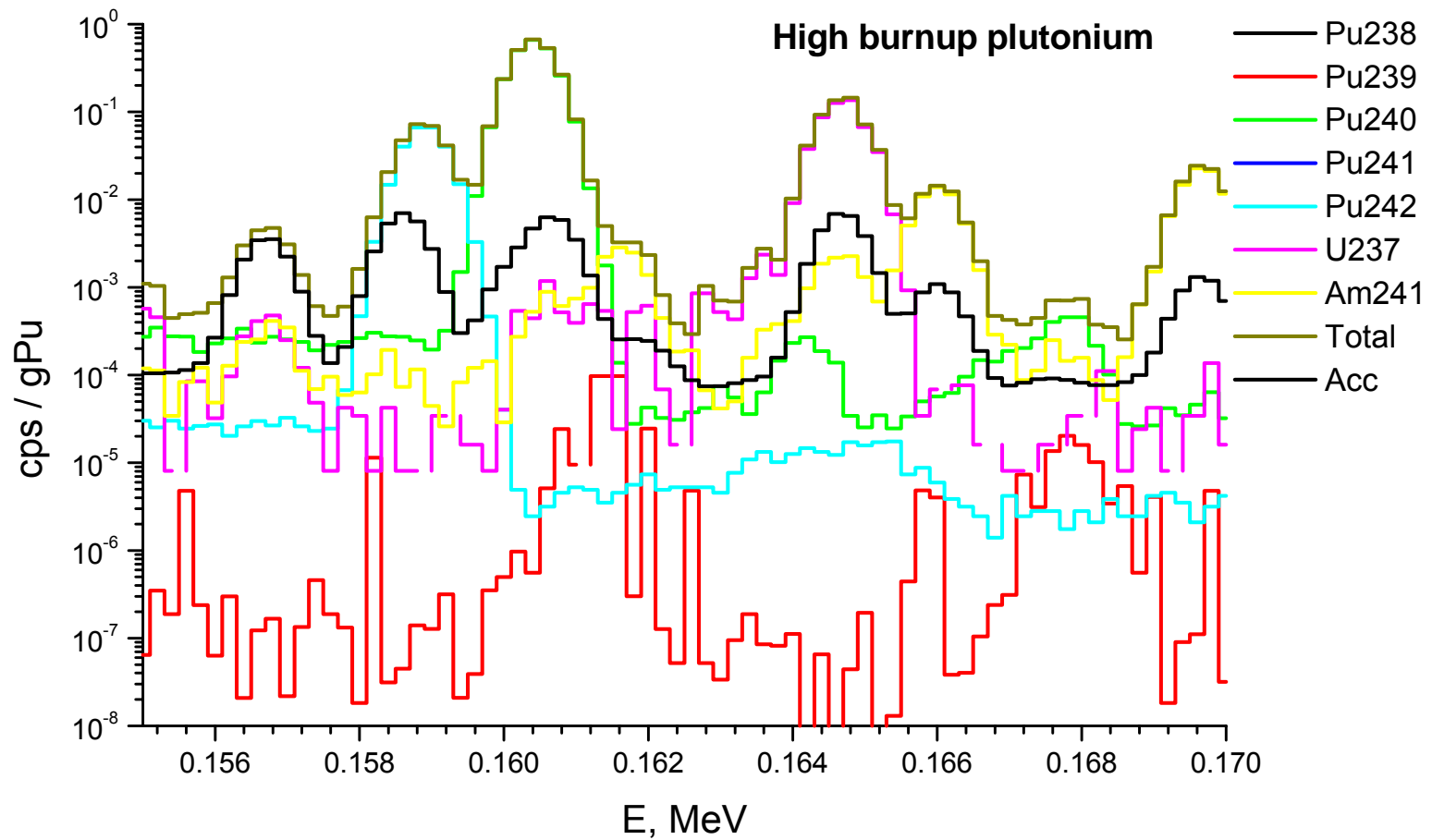
Other parameters:

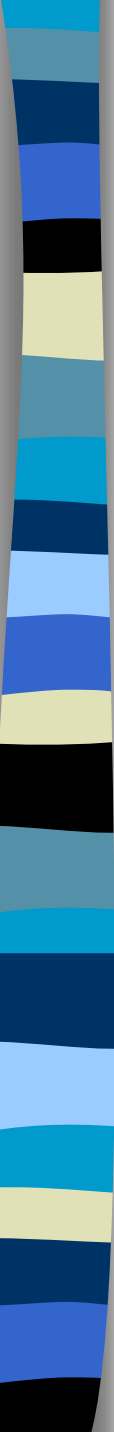
- $\text{FWHM}=a+b*E^{1/2}$, $\text{FWHM}(5.9 \text{ keV})=300 \text{ eV}$, $\text{FWHM}(122 \text{ keV})=600 \text{ eV}$.
- LBU Pu: 0.0109% ^{238}Pu , 93.54% ^{239}Pu , 6.292% ^{240}Pu , 0.1149% ^{241}Pu , 0.0385% ^{242}Pu , 0.201% ^{241}Am (Pu-2000 Sample M).
- HBU Pu: 1.303% ^{238}Pu , 64.99% ^{239}Pu , 24.02% ^{240}Pu , 5.041% ^{241}Pu , 4.642% ^{242}Pu , 4.95% ^{241}Am (Pu-2000 Sample N).

Direct spectra: ROIs



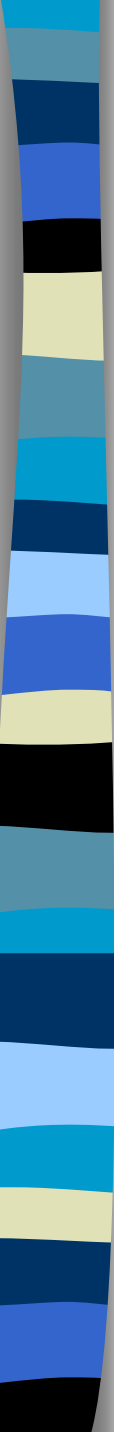
Results: coincidence spectrum





Summary

- A standard MCNP code was extended to allow carrying out calculations with a radiation source emitting correlated nuclear particles.
- A new version of the code, MCNP-CP, performs statistical simulation of processes accompanying radioactive decay of a specified radionuclide, yielding characteristics of emitted correlated nuclear particles, which are then transported through the problem geometry.
- MCNP-CP presents a powerful tool for predicting responses and performance characteristics of conventional single detector as well as advanced multi-detector γ - and β -spectrometry systems.



Thank you for your attention !